SURFACE CURRENTS IN CHIRAL P-WAVE SUPERCONDUCTORS

SURFACE CURRENTS IN CHIRAL P-WAVE SUPERCONDUCTORS

By

PHILLIP E. C. ASHBY, B.Sc.

A Thesis
Submitted to the School of Graduate Studies
in Partial Fulfillment of the Requirements
for the Degree
Master of Science

McMaster University

MASTER OF SCIENCE (2008)
(Physics)

McMaster University
Hamilton, Ontario

TITLE: Surface Currents in Chiral p-Wave Superconductors

AUTHOR: Phillip E. C. Ashby, B.Sc.(University of Calgary)

SUPERVISOR: Dr. C. Kallin

NUMBER OF PAGES: vii, 37

Abstract

It is believed that Sr_2RuO_4 is a triplet superconductor that breaks time reversal symmetry, and it is expected to have spontaneous magnetization both at the sample edge, as well as at domain walls. Recent magnetic microscopy results place upper limits on the magnetic fields differing from previous theoretical calculations by 2 orders of magnitude. Using a Ginzburg-Landau formalism we investigate the effects of a rough surface as well as parameter choices which differ from the typical weak coupling parameters on the magnitudes of the spontaneous supercurrents and magnetic fields. The dependance on surface roughness is found to be small resulting in only a 20% reduction for the weak coupling parameters. Changing the parameters from weak coupling in addition to pair breaking surface effects is also found to affect the magnitudes of the spontaneous fields weakly, except in certain unphysical parameter regimes. The effects of the surface stabilizing another non-magnetic order parameter are considered, and give rise to field distributions with similar features to those present at domain walls.

Acknowledgements

I am grateful to my supervisor, Dr. Catherine Kallin, both for suggesting this research topic and for her guidance over the past two years. I would also like to thank the other members of my committee Drs. John Berlinsky and Erik Sorensen for reading this thesis on such short notice.

There are a number of other grad students that have made McMaster a more enjoyable place. My office-mates Mike Young and Eric Mills have provided much discussion, both of the intelligible and unintelligible varieties. The late nights working with Josh McGraw, Prasanna Balasubramanian and Marc-Antoni Goulet on condensed matter assignments created a special bond between very different people. I could always go to Prasanna for a discussion on physics, Josh for the much needed beer and games of crib, and Marc always kept things interesting. I'd like to thank Clare Armstrong for creating and diffusing more awkward situations than she needed to. Finally thanks to Patrick Rogers and Josh McGraw for trying to keep my mind off science by enforcing "no shop talk", and Allan Bayntun for always wanting to talk shop, no matter the circumstances.

Lastly, I would like to thank my parents, for never telling me that asking "why?" was silly. This is without a doubt the reason for my interest in the sciences.

CONTENTS

LIST OF FIGURES

CHAPTER 1

Introduction

The phenomenon of superconductivity is a phase transition to a state characterized by both perfect conductivity and perfect diamagnetism. This state is well investigated, and has been understood as an instability of the Fermi-liquid state in the presence of an attractive interaction. In the presence of such an interaction the electrons tend to form *Cooper pairs*, leading to the formation of a condensate of the paired electrons. Along with the phase transition comes the formation of an energy gap, Δ, an energy cost for exciting quasi-particles from the ground state. In conventional superconductors, the attraction is mediated by the electron-phonon interaction, and occurs in the lowest angular momentum state (s-wave). In 1965 a paper by Kohn and Luttinger showed that a weak attractive interaction between electrons could be generated through the Coulomb repulsion through higher angular momentum channels [1]. Although the unconventional superfluid He-3 was discovered in 1972, its electronic analogues went undiscovered for many years. We presently know of many such systems. Among the unconventional superconductors are heavy fermion materials, organic compounds, high T_c cuprates, and strontium ruthenate, Sr_2RuO_4, which is the material that is the focus of this thesis.

1.1 Notation

A useful model that describes the superconducting phase transition was developed by Ginzburg and Landau (GL) in 1950 [2]. According to the GL theory of phase transitions, we express the free energy of a system undergoing a phase transition as a power series in an *order parameter* [3]. Although originally phenomenological in its design, the GL model was shown to be a limiting case of the microscopic theory in 1959, by Gor'kov [4], with the superconducting order parameter proportional to the complex energy gap. Physically we can think of the order parameter as the wavefunction for

the center of mass coordinate of the Cooper pairs which form the superconducting state, with the magnitude squared of the order parameter as the density of superconducting electrons.

Since the order parameter is what characterizes the phase transition, it is useful to introduce some notation which is common in describing it. Writing the pair wavefunction, ψ, as an orbital part times a spin part, we have $\psi = f(\mathbf{k})\chi_{ab}$. Since electrons obey Fermi statistics, by considering the exchange of electrons in a pair we have

$$f(\mathbf{k})\chi_{ab} = -f(-\mathbf{k})\chi_{ba}. \tag{1.1}$$

The Cooper pairs are formed from two spin $\frac{1}{2}$ particles and we can construct the total spin wavefunction starting from the eigenstates of the single particle operators:

$$|\uparrow\rangle = \begin{pmatrix} 1 \\ 0 \end{pmatrix} \quad \text{and} \quad |\downarrow\rangle = \begin{pmatrix} 0 \\ 1 \end{pmatrix}. \tag{1.2}$$

The resultant total spin states will have total spin eigenvalue 0 or 1, conventionally denoted by spin singlet and spin triplet states respectively. The spin singlet wavefunction is given by

$$\psi = f(\mathbf{k})\left(|\uparrow\downarrow\rangle - |\downarrow\uparrow\rangle\right) \tag{1.3}$$

and the spin triplet state is in general a superposition of the three states with total spin 1, namely

$$\psi = g_1(\mathbf{k})\,|\uparrow\uparrow\rangle + g_2(\mathbf{k})(|\uparrow\downarrow\rangle + |\downarrow\uparrow\rangle) + g_3(\mathbf{k})\,|\downarrow\downarrow\rangle\,. \tag{1.4}$$

We see that the spin part of the singlet state is odd under the exchange of the two particles, while that of the triplet state is even under exchange. The Fermi principle, Eq. 1.1, gives that orbital part of the spin singlet states must have even parity, while triplet states have orbital wavefunctions with odd parity. Since we are explicitly considering the spin of the wavefunction, it is convenient to represent it as a martix in spin space:

$$\hat{\psi}(\mathbf{k}) = \begin{pmatrix} \psi(\mathbf{k})_{\uparrow\uparrow} & \psi(\mathbf{k})_{\uparrow\downarrow} \\ \psi(\mathbf{k})_{\downarrow\uparrow} & \psi(\mathbf{k})_{\downarrow\downarrow} \end{pmatrix} \tag{1.5}$$

In this notation, a spin singlet state is given by

$$\hat{\psi}(\mathbf{k}) = \begin{pmatrix} 0 & f(\mathbf{k}) \\ -f(\mathbf{k}) & 0 \end{pmatrix} = f(\mathbf{k})i\sigma_y, \tag{1.6}$$

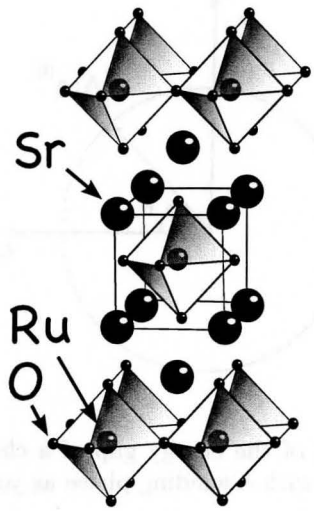

Figure 1.1: A portion of the crystal structure of Sr_2RuO_4. The RuO octahedra define a series of stacked two dimensional planes in which the electronic action takes place.

where $f(\mathbf{k})$ is even in $\mathbf{k}$, and σ_y is the usual Pauli matrix. For a spin triplet we have

$$\hat{\psi}(\mathbf{k}) = \begin{pmatrix} g_1(\mathbf{k}) & g_2(\mathbf{k}) \\ g_2(\mathbf{k}) & g_3(\mathbf{k}) \end{pmatrix}, \tag{1.7}$$

where the $g(\mathbf{k})$ are odd in $\mathbf{k}$. It is common in the literature to use a slightly different notation, introducing a vector, $\mathbf{d(k)}$, defined by

$$\hat{\psi}(\mathbf{k}) = (\mathbf{d}(\mathbf{k}) \cdot \boldsymbol{\sigma})\, i\sigma_y = \begin{pmatrix} -d_x(\mathbf{k}) + id_y(\mathbf{k}) & d_z(\mathbf{k}) \\ d_z(\mathbf{k}) & d_x(\mathbf{k}) + id_y(\mathbf{k}) \end{pmatrix}. \tag{1.8}$$

Here $\boldsymbol{\sigma}$ is the vector of Pauli matrices

$$\boldsymbol{\sigma} = \begin{pmatrix} \sigma_x \\ \sigma_y \\ \sigma_z \end{pmatrix}. \tag{1.9}$$

Thus, we have that the function $f(k)$ specifies the superconducting state for singlet systems, while the vector function $\mathbf{d}(\mathbf{k})$ defines the superconducting state for triplet systems.

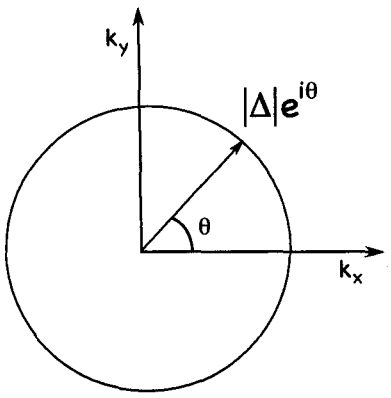

Figure 1.2: Pictorial representation of the energy gap of a chiral p-wave superconductor showing that it has constant magnitude but with a winding phase as you move around the Fermi surface.

1.2 Strontium Ruthenate

Strontium ruthenate was discovered to be a superconductor in 1994 [5], and has since attracted considerable experimental and theoretical study. It has a layered two dimensional structure as shown in Fig. 1.1, with the Ru-O planes separated by Sr. These two dimensional planes are weakly coupled to each other, and the electronic behaviour is essentially 2 dimensional. This structure is the same as that of the high-T_c cuprates, although Sr_2RuO_4 has a transition temperature which is actually low, coming in at $T_c \approx 1.5$K for high quality samples.

Early evidence which pointed towards strontium ruthenate as an unconventional superconductor was the sensitivity of the superconducting transition temperature to sample quality. For conventional superconductors Anderson proved a theorem that they should have a T_c which is robust against disorder [6]. Many experiments were done to attempt to classify the superconducting order in strontium ruthenate: NMR experiments [7, 8], neutron scattering [9] as well as phase sensitive Josephson measurements [10] have all been interpreted as evidence for spin triplet pairing. There have also been a number of experiments, including muon spin resonance and more recently the Kerr effect, demonstrating that the superconducting phase shows weak magnetic signatures [11, 12, 13, 14].

The superconducting state was proposed early on by Rice and Sigrist [15] to be an analogue of the A phase of superfluid He-3 [16]. This state is known as a chiral p-wave, $\mathbf{d} = (p_x \pm ip_y)\hat{\mathbf{z}}$,[1] and is considered the simplest state consistent with most experiments [17]. Depicted in Fig. 1.2, this state has a constant magnitude $|\Delta| = \sqrt{p_x^2 + p_y^2}$, but with a continuously winding phase to satisfy the odd parity requirements demanded by Fermi statistics. There are two directions in which the phase can wind, and these correspond to two distinct chiralities associated with the energetically equivalent states $p_x + ip_y$ and $p_x - ip_y$. The chirality of these states is physically related to the

[1] we will omit the spin space vector and simply refer to this state as $p_x \pm ip_y$

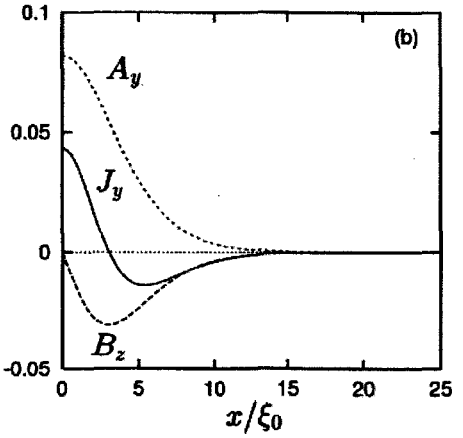

Figure 1.3: The predicted current and field distributions at the edge of a chiral p-wave superconductor. Taken from Matumoto and Sigrist [20].

angular momentum and is given by $\pm\hbar$ per Cooper pair.

A result of this chirality is the expectation that there should be spontaneous supercurrents flowing around the sample edge [18, 19, 20, 21]. To understand this it is useful to think of each electron pair as a small current loop: while neighbouring loops cause the contribution to the total current to cancel in the bulk, at the edge of the sample these currents will add to create a current which flows around the sample with its direction given by the chirality of the superconducting state. This current is then screened by the Meissner effect so that the magnetic field is zero inside the superconductor. The result of a calculation done by Matsumoto and Sigrist [20] is given in Fig. 1.3 showing the spontaneous current which is predicted at the sample edge as well as the magnetic field. The net result is a magnetic field confined near the edge of the sample.

As mentioned above, the two chiralities are energetically degenerate and we may expect domain walls to form between $p_x + ip_y$ and $p_x - ip_y$ domains. Spontaneous currents and fields will also occur within the sample at such domain walls and have been studied by Matsumoto and Sigrist as well as others[22, 21, 20, 23, 19] and should be observable by scanning probe measurements [24]. As well, muon spin resonance experiments have been interpreted as evidence for internal fields present at domain walls[11, 12].

Recent scanning Hall bar and superconducting quantum interference device (SQUID) microscopy measurements did not see the expected signatures of spontaneous currents at the sample edges and surfaces.[25, 26] These null measurements set upper limits on the spontaneous currents and are approximately two orders of magnitude smaller than the values predicted from simple chiral p-wave order.[26] Fig. 1.4 shows the predicted magnetic signal as well as the one measured by Kirtley *et al.* [26].

Given the considerable body of experimental results taken as evidence for chiral p-wave order,

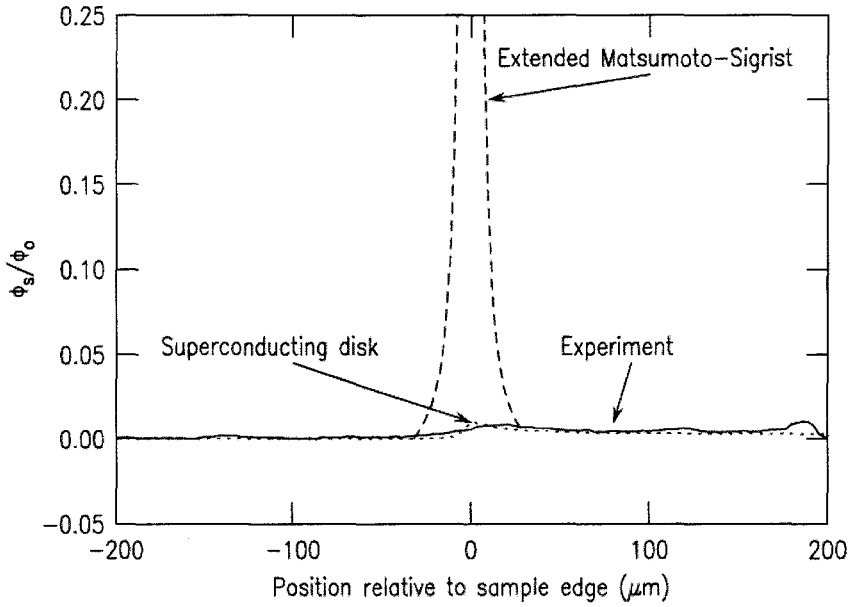

Figure 1.4: Comparison of the experimental results for spontaneous edge currents and the predictions based on the self-consistent calculations of Matsumoto and Sigrist. Taken from Kirtley *et al.* [26].

it is important to understand whether the absence of observable magnetization at the edges can be explained within a theory of bulk chiral p-wave superconductivity. One possibility discussed by Kirtley *et al.*[26] is domains at the surface smaller than 1 or 2 microns on average. Given the size of the experimental probes, this could account for the null results.[26] Indeed, Josephson tunneling measurements were interpreted as evidence of chiral p-wave order with small dynamic domains,[13] although other results would be incompatible with such small domains at the surface[10, 14] or in the bulk[10]. The formation of domain walls is energetically unfavorable and the samples are considered clean (otherwise T_c is noticeably reduced as expected for unconventional pairing[27]), so such small domains are unlikely. Additional experiments are required to either rule out or confirm this possibility.

Previous work [20, 23] on the spontaneous currents have only considered ideal surfaces (specular scattering). One might expect surface roughness or other surface effects to reduce the spontaneous currents. Previous studies on neutral superfluids which included the effect of rough surfaces had been modeled in the Bogoliubov-de Gennes (BdG) formalism or the closely related Greens function formalism.[28]

The goal of this thesis is to investigate surface effects in a chiral p-wave superconductor, where there are screening currents present. We use a Ginzburg-Landau (GL) formalism allowing us to study the effect of a variety of surfaces as the parameters in the theory are varied. These correspond

to studying different microscopic Hamiltonians in the BdG formalism, which each stabilize a $p_x \pm ip_y$ superconductor. The BdG formalism is more accurate at low temperatures, although for specular surfaces it was found that the GL calculations gave qualitatively similar results for the spontaneous currents and fields.[20, 23] Lastly we consider the effect of surfaces which nucleate a non-chiral order parameter, while maintaining $p_x \pm ip_y$ in the bulk, as a possible mechanism for suppressing the predicted edge currents.

CHAPTER 2

Constructing the Free Energy

To construct the free energy according to the GL recipe, we require that it be invariant under the symmetries of the problem at hand. For a given symmetry group $\mathcal{G}$, we can express any property of the system as a sum of coefficients times scalars formed from the basis functions of the irreducible representations (irreps) of $\mathcal{G}$. As the temperature of the system is lowered, the system undergoes a phase transition and the coefficients for one of the irreps becomes non-zero. In general, the transition temperatures are different for different irreps, and the one with the largest transition temperature describes the phase transition. The free energy is then constructed as a sum of invariants of this irrep, which are tabulated in books on group theory [29] or review articles [21]. The reader interested in more group theory can consult either of the standard texts of Tinkham [30] or Landau and Lifshitz chapter 14 [3].

It is useful to first consider the superconductor in the absence of the crystal field and spin-orbit coupling. In this case the problem is spherically symmetric and as we know the spherical harmonics are the basis function of the group of rotations. Expanding the $f(\mathbf{k})$ and $\mathbf{d}(\mathbf{k})$ we have:

$$f(\mathbf{k}) = \sum_{m=-l}^{l} a_{lm} Y_{lm}(\hat{\mathbf{k}}), \qquad l = 0, 2, \cdots, \tag{2.1}$$

$$\mathbf{d}(\mathbf{k}) = \sum_{m=-l}^{l} \mathbf{a}_{lm} Y_{lm}(\hat{\mathbf{k}}), \qquad l = 1, 3, \cdots, \tag{2.2}$$

where the restriction on l follows from the fact that the f are even and the $\mathbf{d}$ are odd. In each of Eqs. 2.1 and 2.2 the coefficients a_{lm} play the role of the superconducting order parameter. For a simple s-wave ($l = 0$) we see that there is only one component a_{00} which specifies the superconducting state. The simplest spin triplet state ($l = 1$) has 9 functions which specify the system, and is usually

Table 2.1: Irreps for D_{4h} with odd basis functions

Representation	Basis Function(s)	Dimension
Γ_1^-	$k_x\hat{\mathbf{x}} + k_y\hat{\mathbf{y}}$	1
Γ_2^-	$k_y\hat{\mathbf{x}} - k_x\hat{\mathbf{y}}$	1
Γ_3^-	$k_x\hat{\mathbf{x}} - k_y\hat{\mathbf{y}}$	1
Γ_4^-	$k_y\hat{\mathbf{x}} + k_x\hat{\mathbf{y}}$	1
Γ_5^-	$k_x\hat{\mathbf{z}}, k_y\hat{\mathbf{z}}$	2

represented as a 3×3 matrix in the He-3 literature where there is indeed spherical symmetry.

In the presence of the crystal field and spin orbit coupling, angular momentum and spin are no longer good quantum numbers. For spin orbit coupling we imagine turning the interaction on adiabatically. This causes the spin states to evolve continuously into two new states labeled instead by "pseudo-spin"; we identify these new states using our old notation $|\uparrow\rangle$ and $|\downarrow\rangle$. Since the crystal breaks the continuous group of rotations into a finite point group, there are now a finite number of irreps (commonly denoted by Γ) which describe the symmetry of the system. The basis functions of the irreps for all of the point groups are tabulated and can be found in reference [29]. The expressions for the spatial wave function for a representation Γ, of dimension d, now take the form

$$f(\mathbf{k}) = \sum_{m=1}^{d} b_i \eta_i^{\Gamma}(\hat{\mathbf{k}}) \tag{2.3}$$

for spin singlet pairing, and

$$\mathbf{d}(\mathbf{k}) = \sum_{m=1}^{d} b_i \boldsymbol{\eta}_i^{\Gamma}(\hat{\mathbf{k}}) \tag{2.4}$$

for spin triplet pairing. Here, the basis functions $\boldsymbol{\eta} = \eta_x(\hat{\mathbf{k}})\hat{\mathbf{x}} + \eta_y(\hat{\mathbf{k}})\hat{\mathbf{y}} + \eta_z(\hat{\mathbf{z}})\hat{\mathbf{z}}$ are vectors in spin space. In Eq.'s 2.3 and 2.4 the coefficients b_i play the role of the order parameters.

For strontium ruthenate the point group is given by D_{4h}, there is spin orbit coupling, and the experimental evidence points towards triplet pairing. There are only 5 irreducible representations who's basis functions are odd, and these are listed in Table 2.1. All of these irreps have a much lower dimension than the higher symmetry case, and we will have at most a 2 component order parameter.

CHAPTER 3

The Free Energy and Equations of Motion

Since strontium ruthenate has the point group D_{4h}, there is only one irrep which is compatible with producing magnetic signatures. This is the two-dimensional representation of D_{4h} as no one component order parameter can describe a magnetic superconducting state [31]. We require the free energy to be invariant under the $U(1)$ gauge symmetry as well as time reversal symmetry ($\mathcal{T}$). The most general free energy transforming under $D_{4h} \times U(1) \times \mathcal{T}$:

$$\begin{aligned} F = \int d^3r' \Big[& A(T)\left(|\psi_x|^2 + |\psi_y|^2\right) + \beta_1\left(|\psi_x|^2 + |\psi_y|^2\right)^2 + \beta_2\left(\psi_x^*\psi_y - \psi_x\psi_y^*\right)^2 + \beta_3\left(|\psi_x|^2|\psi_y|^2\right) \\ & + K_1\left(|D_x\psi_x|^2 + |D_y\psi_y|^2\right) + K_2\left(|D_y\psi_x|^2 + |D_x\psi_y|^2\right) + K_3\left((D_x\psi_x)^*(D_y\psi_y) + \text{c.c.}\right) \\ & + K_4\left((D_y\psi_x)^*(D_x\psi_y) + \text{c.c.}\right) + \frac{1}{8\pi}\mathbf{B}^2 \Big], \end{aligned} \tag{3.1}$$

where $D_i = \frac{\partial}{\partial x_i} - \frac{2ie}{\hbar c}A_i$ are the usual gauge covariant derivatives. Note here that we use the convention $e = -|e|$, the charge on the electron. In the bulk, the gradient terms vanish as well as the magnetic field. Parameterizing the order parameters by $\psi_x = |\psi_x|e^{i\theta}$ and $\psi_y = |\psi_y|e^{i(\theta+\phi)}$ gives the following equations of motion:

$$0 = A(T)|\psi_x| + 2\beta_1|\psi_x|^3 + \left(2\beta_1 - 4\beta_2\sin^2(\phi) + \beta_3\right)|\psi_y|^2|\psi_x|, \tag{3.2}$$

$$0 = A(T)|\psi_y| + 2\beta_1|\psi_y|^3 + \left(2\beta_1 - 4\beta_2\sin^2(\phi) + \beta_3\right)|\psi_x|^2|\psi_y|, \tag{3.3}$$

$$0 = |\psi_x|^2|\psi_y|^2\sin(\phi)\cos(\phi). \tag{3.4}$$

The last equation imposes the constraint that $\phi = \frac{n\pi}{2}$. Examination of the free energy gives that for $\beta_2 > 0$, $\phi = \frac{(2n+1)\pi}{2}$ minimizes the free energy, whereas for $\beta_2 < 0$, the choice $\phi = n\pi$ minimizes

the free energy. We focus on the case $\beta_2 > 0$, which stabilizes the chiral p-wave state.

Solving for the order parameters we find $|\psi_x|^2 = |\psi_y|^2 = \frac{-A(T)}{4(\beta_1-\beta_2)+\beta_3} \equiv |\psi_0|^2$ as well as the requirements for the stability of the free energy and the order parameter: $\beta_3 - 4\beta_2 < 0$, and $4(\beta_1 - \beta_2) + \beta_3 > 0$. Now, we use the following definitions we express the free energy in terms of dimensionless quantities. Let $r' = \xi r$, $\mathbf{A}(r') = \sqrt{2}\mathbf{H}_C\lambda\mathbf{a}(r)$ and $(\psi_x, \psi_y) = \psi_0(u, v)$ where

$$\lambda^2 = \frac{c^2}{8\pi(2e)^2(K_1 + K_2)|\psi_0|^2}, \tag{3.5}$$

$$\xi^2 = \frac{4\pi}{\mathbf{H}_C^2}(K_1 + K_2)|\psi_0|^2, \tag{3.6}$$

$$\mathbf{H}_C^2 = \frac{8\pi A^2(T)}{4(\beta_1 - \beta_2) + \beta_3}. \tag{3.7}$$

After some algebra we obtain

$$\begin{aligned} F = \frac{\mathbf{H}_C^2\xi^3}{4\pi}\int d^3r \Big[& -\tfrac{1}{2}\left(|u|^2 + |v|^2\right) + \left(\tfrac{1}{8} + \tfrac{1}{2}b_2\right)\left(|u|^2 + |v|^2\right)^2 + \tfrac{1}{2}b_2\left(u^*v - uv^*\right)^2 \\ & - \tfrac{1}{8}b_3\left(|u|^2 - |v|^2\right)^2 + k_1\left(|d_x u|^2 + |d_y v|^2\right) + k_2\left(|d_y u|^2 + |d_x v|^2\right) \\ & + k_3\left((d_x u)^*(d_y v) + \text{c.c.}\right) + k_4\left((d_x v)^*(d_y u) + \text{c.c.}\right) + \kappa^2\left(\nabla\times\mathbf{a}\right)^2\Big], \end{aligned} \tag{3.8}$$

where we have introduced the following dimensionless quantities : $\kappa = \frac{\lambda}{\xi}$, $\mathbf{d} = \nabla - i\mathbf{a}$, $b_i = \frac{\beta_i}{4(\beta_1-\beta_2)+\beta_3}$, and $k_i = \frac{K_i}{K_1+K_2}$. It is also sometimes convenient to introduce the variables $k_\pm = \frac{1}{2}(k_3 \pm k_4)$. Again, it is convenient to parameterize the order parameters by $u = |u|e^{i\theta}$ and $v = |v|e^{i(\phi+\theta)}$. Choosing the gauge with $\nabla\cdot\mathbf{A} = 0$ and neglecting derivatives in y by symmetry we obtain the following free energy:

$$\begin{aligned} F = \frac{\mathbf{H}_C^2\xi^3}{4\pi}\int d^3r \Big[& -\tfrac{1}{2}\left(|u|^2 + |v|^2\right) + \left(\tfrac{1}{8} + \tfrac{1}{2}b_2\right)\left(|u|^2 + |v|^2\right)^2 - 2b_2|u|^2|v|^2\sin^2(\phi) - \tfrac{1}{8}b_3\left(|u|^2 - |v|^2\right)^2 \\ & + k_1\left[|u|'^2 + |u|^2\theta'^2 + a_y^2|v|^2\right] + k_2\left[|v|'^2 + |v|^2(\theta+\phi)'^2 + a_y^2|u|^2\right] \\ & + 2k_+a_y\left[\sin(\phi)\left(|u|'|v| - |v|'|u|\right) - \cos(\phi)|u||v|\left(2\theta' + \phi'\right)\right] \\ & + 2k_-a_y\left[\cos(\phi)|u||v|\phi' + \sin(\phi)\left(|u|'|v| + |v|'|u|\right)\right] + \kappa^2 a_y'^2\Big]. \end{aligned} \tag{3.9}$$

We now require the free energy to be stationary with respect to variations of u, v, ϕ, θ and a_y to obtain the following equations of motion:

$$
\begin{aligned}
0 =& -k_1|u|'' - (k_+ + k_-)\left(a_y|v|\sin(\phi)\right)' - \tfrac{1}{2}|u| + \left(\tfrac{1}{4} + b_2 - \tfrac{1}{4}b_3\right)|u|^3 \\
&+ \left(\tfrac{1}{4} + b_2\cos(2\phi) + \tfrac{1}{4}b_3\right)|v|^2|u| + k_1|u|\theta'^2 + k_2|u|a_y^2 - k_+\cos(\phi)|v|a_y\left(2\theta' + \phi'\right) \\
&- k_+\sin(\phi)a_y|v|' + k_-\cos(\phi)|v|a_y\phi' + k_-\sin(\phi)a_y|v|', \qquad (3.10) \\
0 =& -k_2|v|'' + (k_+ - k_-)\left(a_y|u|\sin(\phi)\right)' - \tfrac{1}{2}|v| + \left(\tfrac{1}{4} + b_2 - \tfrac{1}{4}b_3\right)|v|^3 \\
&+ \left(\tfrac{1}{4} + b_2\cos(2\phi) + \tfrac{1}{4}b_3\right)|u|^2|v| + k_1|v|a_y^2 + k_2|v|(\theta+\phi)'^2 - k_+\cos(\phi)|u|a_y\left(2\theta' + \phi'\right) \\
&+ k_+\sin(\phi)a_y|u|' + k_-\cos(\phi)|u|a_y\phi' + k_-\sin(\phi)a_y|u|', \qquad (3.11) \\
0 =& -k_2\left(|v|^2(\theta+\phi)'\right)' + (k_+ - k_-)\left(|u||v|a_y\cos(\phi)\right)' - 2|u|^2|v|^2b_2\sin(\phi)\cos(\phi) \\
&+ k_+|u||v|a_y\sin(\phi)\left(2\theta' + \phi'\right) + k_+a_y\cos(\phi)\left(|v||u|' - |u||v|'\right) - k_-|u||v|a_y\sin(\phi)\phi' \\
&+ k_-a_y\cos(\phi)\left(|v||u|' + |u||v|'\right), \qquad (3.12) \\
0 =& -\kappa^2a_y'' + a_y\left(k_1|v|^2 + k_2|u|^2\right) - k_+\cos(\phi)|u||v|\left(2\theta' + \phi'\right) + k_+\sin(\phi)\left(|v||u|' - |u||v|'\right) \\
&+ k_-cos(\phi)|u||v|\phi' + k_-\sin(\phi)\left(|v||u|' + |u||v|'\right), \qquad (3.13) \\
0 =& k_1\left(|u|^2\theta'\right)' + k_2\left(|v|^2(\theta' + \phi')\right)' - 2k_+(\cos(\phi)|u||v|a_y)'. \qquad (3.14)
\end{aligned}
$$

These are the equations to be solved in addition to the Maxwell equation $\frac{4\pi}{c}\mathbf{j} = \nabla\times\nabla\times\mathbf{A}$, which in one dimension reduces to $\frac{4\pi}{c}j_y = -\frac{\partial^2 A_y}{\partial x^2}$. Combining this with Eq. 3.13 gives an equation for the current:

$$
\begin{aligned}
\kappa^2 j_y =& -a_y\left(k_1|v|^2 + k_2|u|^2\right) + k_+\cos(\phi)|u||v|\left(2\theta' + \phi'\right) - k_+\sin(\phi)\left(|v||u|' - |u||v|'\right) \\
&- k_-cos(\phi)|u||v|\phi' - k_-\sin(\phi)\left(|v||u|' + |u||v|'\right) \qquad (3.15)
\end{aligned}
$$

We integrate Eq. 3.14 to obtain:

$$
\theta' = \frac{2k_+\cos(\phi)|u||v|a_y - k_2|v|^2\phi'}{k_1|u|^2 + k_2|v|^2}. \qquad (3.16)
$$

This equation is then used in Eq.'s 3.10-3.13 to reduce the problem to the solution of 4 coupled equations.

The parameters in free energy 3.8 can be derived from a weak coupling BCS Hamiltonian with d-vector aligned along $\hat{\mathbf{z}}$ as in Furusaki *et al.*[23]. The corresponding parameters are $b_2 = \frac{1}{8}$, $b_3 = 0$, $k_1 = \frac{3}{4}$, $k_2 = \frac{1}{4}$, $k_3 = \frac{1}{4}$ and $k_4 = \frac{1}{4}$. We take $\lambda = 190$ nm and $\xi = 66$ nm as parameters appropriate for strontium ruthenate, unless noted otherwise.

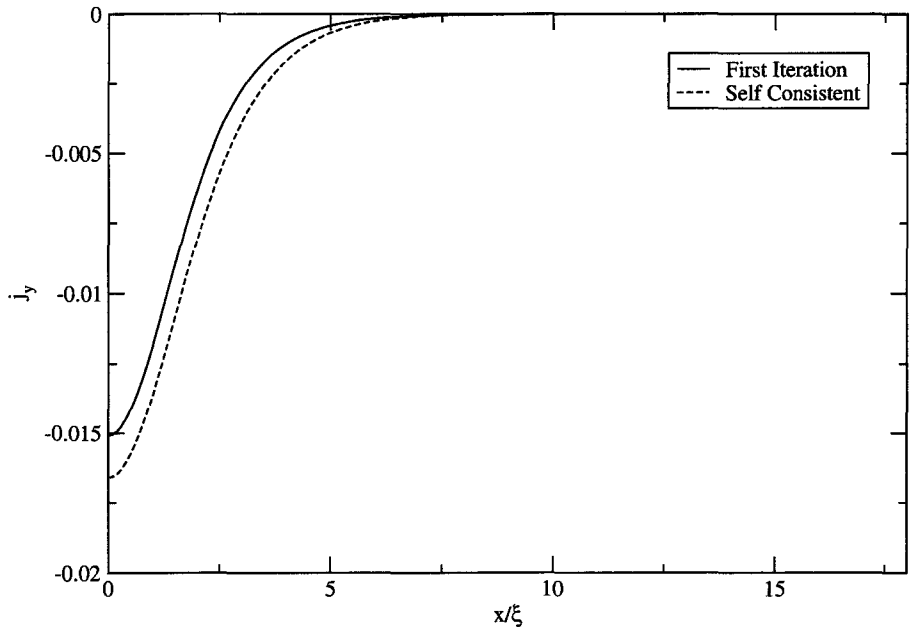

Figure 3.1: The current from Eq. 3.18 and the self consistent current for weak coupling parameters. The currents are scaled by $\frac{\hbar c^2}{8\pi e\xi^3}$.

3.1 Analysis of the Ginzburg-Landau Equations

Some insights can be gained by investigating the Eqs. 3.10-3.13. First, to gain a qualitative understanding we can treat the vector potential as a higher order effect and study a simpler form of the Ginzburg-Landau Equations. As a first approximation we take $v \equiv 1$ and $a_y \equiv 0$ and obtain the following equation for u:

$$\frac{k_1}{\alpha}|u|'' + |u| - |u|^3 = 0 \tag{3.17}$$

with $\alpha = (\frac{1}{4} + b_2 - \frac{1}{4}b_3)$. With the boundary conditions $|u(\infty)|' = 0$, and $|u(0)| = 0$ Eq. 3.17 can be integrated and we obtain the solution $|u| = \tanh\left(x\sqrt{\frac{\alpha}{2k_1}}\right)$. This expression can be substituted into the equation for the current to obtain

$$j_y = \frac{-k_+}{\kappa^2}\sqrt{\frac{\alpha}{2k_1}}\left(1 - \tanh^2\left(x\sqrt{\frac{\alpha}{2k_1}}\right)\right). \tag{3.18}$$

In Fig. 3.1 the approximate solution for the spontaneous current is plotted alongside the self-consistent solution from the algorithm described in the next chapter. The qualitative agreement of the two curves is excellent, although the one given by Eq. 3.18 underestimates the magnitude of

the current at the edge. This agreement gives us confidence that we can use Eq. 3.18 as a good description of the current.

The behaviour of $|v|$ at the surface is less transparent as one must go beyond the constant solution discussed above, but a few quick facts can be obtained from the equations of motion. Again, ignoring the terms proportional to the vector potential, we have:

$$0 = -k_2|v|'' - \tfrac{1}{2}|v| + \alpha|v|^3 + (\tfrac{1}{2} - \alpha)|u|^2|v| \tag{3.19}$$

Evaluating this at $x = 0$ with our specular boundary condition $v'(0) = 0$, we have $v(0) = \sqrt{\frac{1}{2\alpha}}$. For the weak coupling parameters, this gives $v(0) = \sqrt{\frac{4}{3}} \approx 1.155$ in excellent agreement with the self consistent solution $v(0) = 1.152$. This demonstrates that v takes a magnitude different than 1 at the surface. In addition, as u tends towards its bulk value, the coupling term $\left(\frac{1}{2} - \alpha\right)|u|^2|v|$ will become more important. If $\left(\frac{1}{2} - \alpha\right) > 0$ we see that v becomes larger as $u \to 0$, whereas $\left(\frac{1}{2} - \alpha\right) < 0$ gives that v is decreased as $u \to 0$.

Before turning to the GL solutions we first consider the necessary conditions for the current to vanish for the hard wall boundary problem. One can see that the equation for ϕ, Eq. 3.12, is solved by the choice $\phi(x) = \frac{\pi}{2}$. This solution keeps the phase fixed from its bulk value as we move towards the edge, and numerical simulations for a range of parameters indicate that unless ϕ is fixed to a specific value at the edge by a boundary condition that this choice minimizes the free energy.

Using this, we set $a_y \equiv 0$ to determine the conditions that the current vanishes and the equations of motion simplify greatly. We find that there are two ways to obtain $j_y \equiv 0$. First, we can have $|u|' \equiv |v|' \equiv 0$ and substitution of this into the u and v equations of motion immediately leads to the condition $4b_2 - b_3 = 0$. To find the other conditions for $j_y \equiv 0$, we define $\mu = \ln|u|$ and $\nu = \ln|v|$, and the equations of motion can be written:

$$-k_1\left(\mu'' + \mu'^2\right) - \tfrac{1}{2} + \alpha e^{2\mu} + \left(\tfrac{1}{2} - \alpha\right)e^{2\nu} = 0, \tag{3.20}$$

$$-k_2\left(\nu'' + \nu'^2\right) - \tfrac{1}{2} + \alpha e^{2\nu} + \left(\tfrac{1}{2} - \alpha\right)e^{2\mu} = 0, \tag{3.21}$$

$$\frac{k_3}{k_4}\mu = \nu. \tag{3.22}$$

Making use of Eqn. 3.22 we obtain two equations for μ. What follows will derive the consistency conditions on these equations. The equations are:

$$-k_1\left(\mu'' + \mu'^2\right) - \tfrac{1}{2} + \alpha e^{2\mu} + \left(\tfrac{1}{2} - \alpha\right)e^{2\frac{k_3}{k_4}\mu} = 0,$$

$$-\frac{k_2k_3}{k_4}\left(\mu'' + \tfrac{k_3}{k_4}\mu'^2\right) - \tfrac{1}{2} + \alpha e^{2\frac{k_3}{k_4}\mu} + \left(\tfrac{1}{2} - \alpha\right)e^{2\mu} = 0$$

Rearranging these for μ'' and subtracting them gives an equation of constraint:

$$\mu'^2\left[\frac{k_3}{k_4}-1\right]+\tfrac{1}{2}\left[\frac{k_4}{k_3k_2}-\frac{1}{k_1}\right]-e^{2\frac{k_3}{k_4}\mu}\left[\frac{k_4\alpha}{k_3k_2}+\frac{\alpha-\frac{1}{2}}{k_1}\right]+e^{2\mu}\left[\frac{k_4\left(\alpha-\frac{1}{2}\right)}{k_3k_2}+\frac{\alpha}{k_1}\right]=0. \tag{3.23}$$

Now, we take the derivative of this equation and use of one of the equations of motion (either one will do) to eliminate the μ'' term. Collecting terms we obtain:

$$\mu'^2\left[1-\frac{k_3}{k_4}\right]+\tfrac{1}{2}\left[\frac{1}{k_1}-\frac{k_4}{k_3k_2}\right]-e^{2\frac{k_3}{k_4}\mu}\left[\frac{\alpha}{k_2}+\frac{2k_3\left(\alpha-\frac{1}{2}\right)}{k_4k_1}-\frac{\alpha-\frac{1}{2}}{k_1}\right]+e^{2\mu}\left[\frac{k_4\left(\alpha-\frac{1}{2}\right)}{k_3k_2}+\frac{k_3\alpha}{k_1k_4}\right]=0. \tag{3.24}$$

Requiring these equations to be consistent with each other gives two solutions, one solution with $k_1 = k_2$ and $k_3 = k_4$. This solution gives us $|v| = |u|$ everywhere. The other solution is given by $k_1 = k_2$, $k_3 = -k_4$ and $\alpha = \frac{1}{2}$. In this solution the parameters conspire to allow $|v| = \frac{1}{|u|}$ everywhere, which we discard as an unphysical solution due to the divergence in v at $x = 0$.

The preceding shows that to make the spontaneous currents vanishingly small we must have $|v| \to |u|$. Since we have $|u(0)| = 0$ by symmetry, we must introduce an effect which suppresses $|v|$ near the surface as well. Our first approach is to consider a surface which is rough on a scale much smaller than the coherence effect.

To model such a surface we follow deGennes [32] and replace our boundary condition with

$$\frac{1}{|v|}\frac{\partial|v|}{\partial x}\bigg|_{x=0}=\frac{1}{b}. \tag{3.25}$$

This boundary condition also ensures that the current flowing through the boundary is zero and reduces to the specular case for $b = \infty$. Previously, Ambegokar *et al.* showed that the limit of diffuse scattering corresponds to the value $b = 0.54$ [33]. We can also consider a completely pair-breaking effect with $b = 0$ which will force v to zero at the surface as well. Physically this could be caused by magnetic scattering at the surface.

CHAPTER 4

Solutions of the GL equations

4.1 Algorithm

To obtain self-consistent solutions to Eqs. 3.10-3.13 we turn to numerical methods of solution. The GL equations were solved numerically using a numerical relaxation algorithm similar to the one described by Thuneberg [34]. In this algorithm we discretize space and replace derivatives by their simplest difference formulae. The equations of motion are of the form $f(x) = 0$ where $f(x)$ represents the discretized differential equation for x. If we denote the solution of this equation by x^*, and our trial solution by x, we can expand about x:

$$0 = f(x^*) = f(x) + f'(x)(x^* - x) + \frac{1}{2}f''(x)(x^* - x)^2 + \cdots, \tag{4.1}$$

This expression is an exact formula for x^*. If we terminate the series at lowest order we have

$$x^* \approx x - \frac{f(x)}{f'(x)}. \tag{4.2}$$

We use this procedure to adjust our guess, x, and as $\frac{f(x)}{f'(x)}$ gets small enough, our solution will converge to x^*. The error between iteration n and $n+1$ each is given by considering the difference of

$$0 = f(x_n) + (x_{n+1} - x_n)f'(x_n), \tag{4.3}$$

$$0 = f(x_n) + (x^* - x_n)f'(x_n) + \frac{1}{2}f''(x)(x^* - x)^2 + \cdots, \tag{4.4}$$

giving

$$x_{n+1} - x^* = \frac{1}{2}\frac{f''(x_n)}{f'(x_n)}(x^* - x_n)^2 + \cdots . \tag{4.5}$$

The error here is given by the error at the previous step squared, and for a good guess the algorithm converges very quickly. We make the further simplification, by following Thuneberg [34], and avoid the computation of the inverse matrix of derivatives by letting $\left[f'(x)\right]^{-1} = -c$, where $c \in \mathbb{R}$. If $|c|$ is too large, the changes at each step take f away from the solution point, and we do not get converence. Bounds on the size of the relaxation parameter c ensuring convergence can be obtained for linear equations, but are unknown in general for nonlinear systems. The value of the relaxation parameter c is then chosen by hand as large as possible to get the quickest convergence. Using this, our procedure for changing the solution is given by

$$0 = f(x_n) - \frac{1}{c}(x_{n+1} - x_n), \qquad \text{or} \tag{4.6}$$

$$x_{n+1} = x_n + cf(x_n). \tag{4.7}$$

When the differential equation is satisfied, $f(x) = 0$ and we have $x_{n+1} = x_n$. This leads us to choose our convergence criterion to be $f(x_n) < \epsilon$ for $\epsilon \ll 1$. Typical values used were $c = 10^{-3}$ and $\epsilon = 10^{-5}$. The value of c was found to depend strongly on the mesh size, with a refinement of a factor of 2 in the mesh corresponding to the requirement that c be a factor of 10 smaller for convergence to be reached.

4.2 Results

The result of a self-consistent solution of Eqs. 3.10-3.13 for the weak coupling parameters is given in Fig. 4.1 for the specular, diffuse and completely pair-breaking boundary condition on v. Notice that the x-component of the order parameter remains almost unchanged for the different boundary conditions, since the boundary condition was already completely pair-breaking for this order parameter. As anticiplated in chapter 3 the y-component of the order parameter becomes larger than it's bulk value as the x-component falls to zero; however, for those boundary conditions which are pair breaking it is ultimately suppressed close to the surface. This behaviour can be attributed to the different healing lengths for the two order parameters in response to a perturbation in x. The magnitude of the spontaneous magnetic fields is reduced, with the integrated magnetic field being about 20% smaller for diffuse scattering and about 60% smaller for the completely pair-breaking case.

To motivate which parameters to change we look to Eq. 3.18 for an idea of the dependance of spontaneous current on the various parameters in the free energy. We see that the current depends

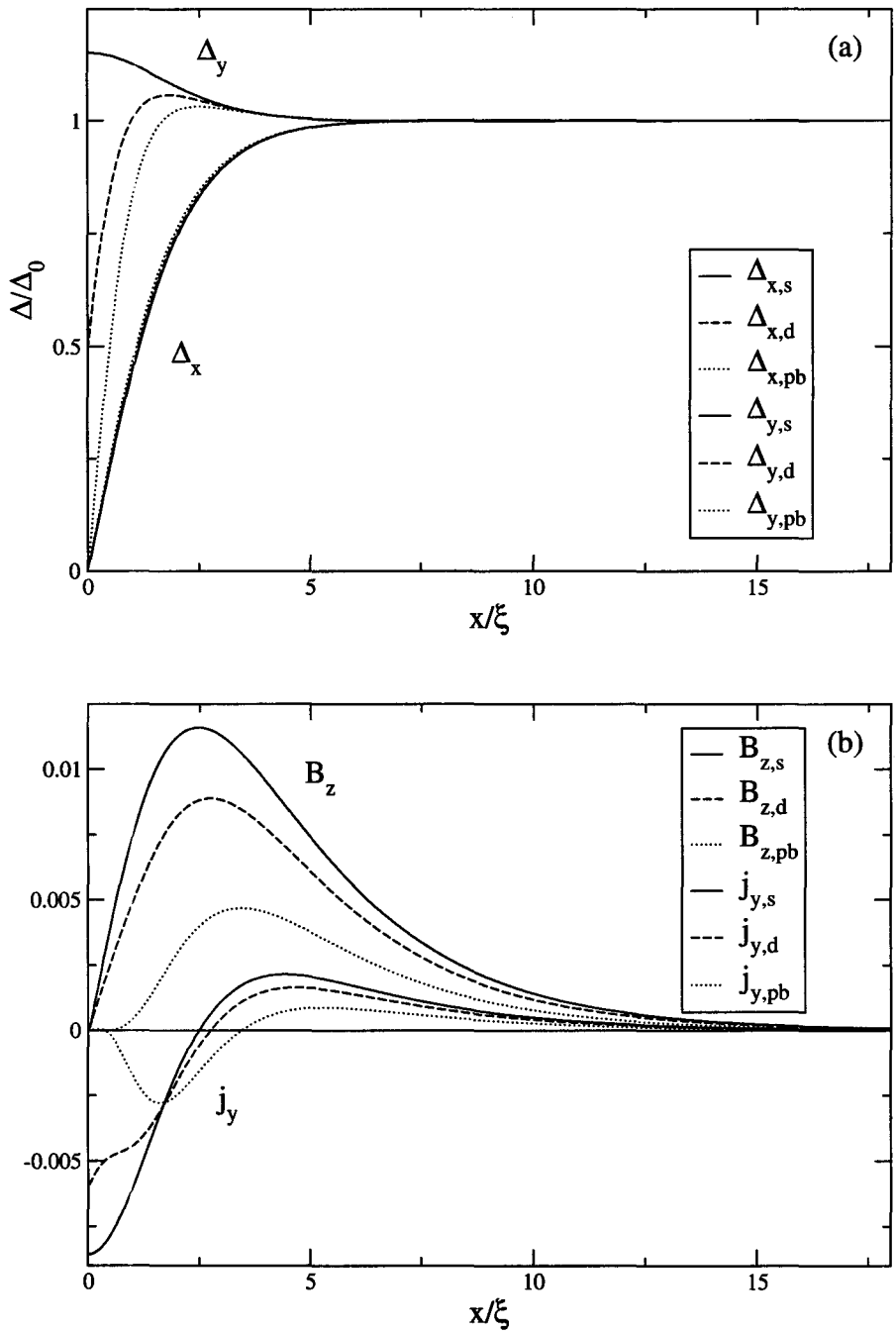

Figure 4.1: Self consistent solution of the Ginzburg-Landau equations for the weak coupling parameters. (a) The x and y components of the order parameters scaled by the bulk order parameter. Here the subscripts s,d and pb denote the case of specular and diffuse scattering, and the pair-breaking boundary condition respectively. (b) The magnetic field and current distributions scaled by $\frac{\hbar c}{2e\xi^2}$ and $\frac{\hbar c^2}{8\pi e\xi^3}$ respectively. A comparison of the integral of the magnetic filed over 25 coherence lengths shows a 22% reduction for the diffuse case compare to specular scattering.

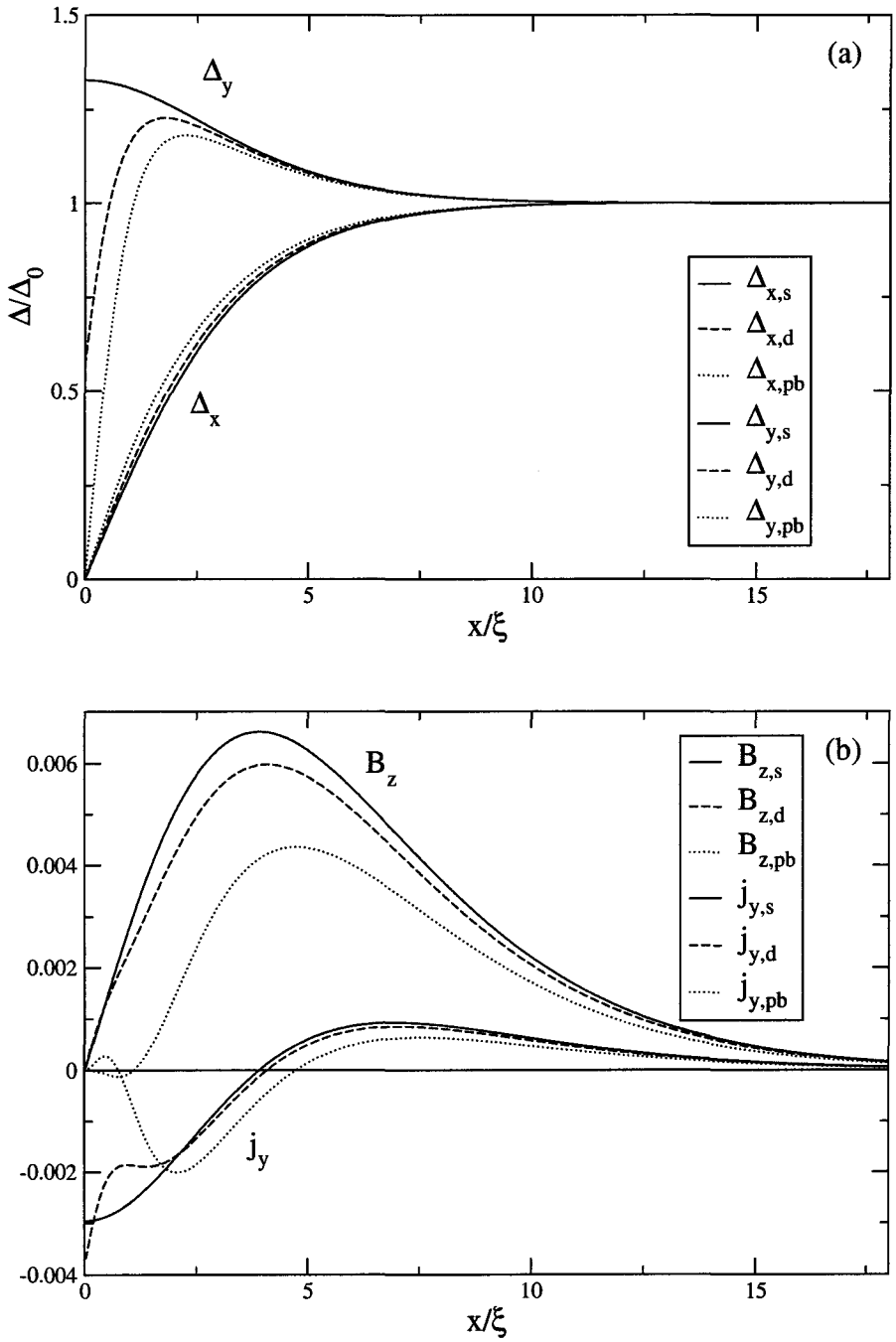

Figure 4.2: Self consistent currents, fields and corresponding order parameters for the parameters $b_2 = \frac{1}{16}$, $b_3 = \frac{1}{8}$, $k_1 = \frac{3}{4}$, $k_3 = \frac{1}{4}$. In this parameter regime the currents and fields are naturally suppressed, with the integrated magnetic field 23% less than that of weak coupling parameters. Also, the changes in the currents and fields due to surface roughness is minimal here resulting in only 10% change in the integrated magnetic field.

on $\sqrt{\alpha}$ and so we expect that the currents will reduce in magnitude as α assumes its smallest value. Recalling that $\alpha = \frac{1}{4} + b_2 - \frac{1}{4}b_3$, as well as the stability condition $4b_2 - b_3 > 0$ we see that the currents being maximally reduced corresponds to the instability of the chiral p-wave state. In fact, as we already saw in chapter 3, the case $j_y \equiv 0$ implies that $4b_2 - b_3 = 0$ (under certain conditions). In Fig. 4.2 we plot the currents and fields from a self-consistent calculation for a smaller value of α than for weak coupling. The field magnitudes are indeed smaller than in weak coupling; however, since a reduction of the currents by this choice of parameters is linked to the stability of the chiral p-wave state, this will reduce all magnetic signatures, and not only those at the edge.

The last set of parameters which can be changed are the coefficients k_i, corresponding to the stiffnesses of the order parameters. As is evident from Eq. 3.18 the magnitude of the current scales linearly with k_+. Furthermore, as we saw in the derivation of the conditions for j_y to vanish, any finite k_- will contribute to the spontaneously generated current. As has been previously pointed out [31] the term proportional to k_- can be re-written as a spontaneous internal magnetization. Thus, it suffices to take $k_- = 0$ when looking for mechanisms which reduce the current.

The last parameters which can be changed are k_1 and k_2. These already satisfy $k_1 + k_2 = 1$ and so it suffices to consider the spontaneous magnetization as a function of $k_1 - k_2$. This dependance is plotted in Fig. 4.3 for the different boundary conditions on the y-component of the order parameter. As expected, the integrated magnetic field is reduced as the two order parameters are forced to vary on the same length scale. For the completely pair-breaking boundary condition the spontaneous magnetization at the edge vanishes for $k_1 = k_2$, as it must.

For the situation at a domain wall it is not obvious that the magnetization should vanish for $k_1 = k_2$. At a domain wall the relative phase of the order parameters can either undergo a discontinuous change, or continuously kink though zero. Previously, Matsumoto and Sigrist showed that the domain wall with the discontinuous phase was energetically favoured.[20] A self consistent solution of the GL equations, shows that for this type of domain wall there are still spontaneously generated magnetic fields. This scenario gives both no edge currents, but while maintaining magnetic signatures attributed to domain walls. However, $k_1 - k_2$ being non-zero reflects the energetic difference between longitudinal and transverse perturbations of the order parameter, which are in general different energetically. Since there is no symmetry in our system to force $k_1 = k_2$, they will in general be different. Another possibility is that as $k_1 - k_2$ is tuned closer to zero, the domain wall with a continuously varying phase becomes stabilized. This domain wall configuration has no spontaneously generated magnetic fields, and will thus not be compatible with the signatures of magnetization in the bulk.

One last feature of Fig. 4.3 which stands out, is the *increase* of the overall magnetic signal for the specular boundary condition as $k_1 \to k_2$. To understand this we express the screening currents

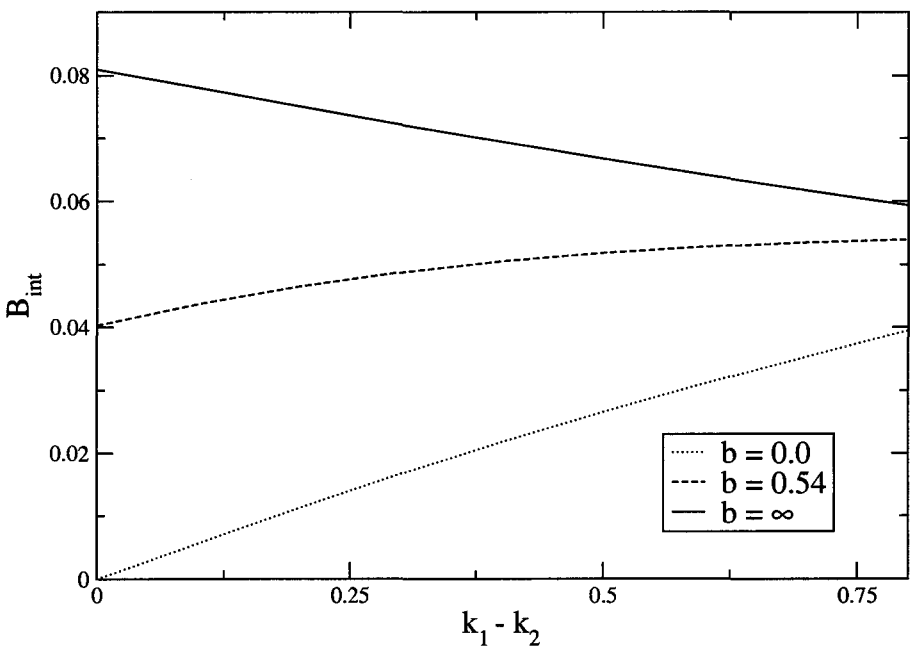

Figure 4.3: Dependence of the integrated magnetic field on the parameter $k_1 - k_2$ for specular and diffuse scattering, and the pair breaking boundary condition, all other parameters are as for weak coupling. The weak coupling parameters for k_1, k_2 correspond to $k_1 - k_2 = \frac{1}{2}$.

(j_s) in terms of the sum and difference of k_1 and k_2:

$$\begin{aligned}\kappa^2 j_s &= -a_y(k_1|u|^2 + k_2|v|^2) \\ &= -\frac{a_y}{2}\left[(k_1+k_2)(|u|^2+|v|^2) + (k_1-k_2)(|v|^2-|u|^2)\right]. \end{aligned} \tag{4.8}$$

From Eq. 4.8 we see that as $k_1 - k_2 \to 0$ the screening currents are reduced in the region where $(|v|^2 - |u|^2) > 0$, which is only satisfied near the sample edge. The change in $k_1 - k_2$ also changes the shape of the spontaneous currents. From Eq. 3.18 we see that the current both increases in magnitude and is pulled closer to the sample edge as k_1 is reduced. This move of the spontaneous currents to the region where the screening currents are reduced results in an increased magnetic signal.

CHAPTER 5

Competing Order Parameters

Another possible surface effect which could cause the spontaneous supercurrents to be suppressed is the nucleation of an order parameter which does not support spontaneous currents at the sample edge. Until now we have assumed that the transition temperatures of the different irreducible representations are well separated so that the superconductor free energy is expressed in terms of a single irreducible representation. When two type of order have close enough transition temperatures, the free energy becomes the most general expression containing both order parameters which transforms under the symmetry group of the problem. To first understand how a sub-dominant order parameter changes the behaviour of the dominant order, we will consider the simpler case of two one component order parameters. As an example we consider the case of an s-wave order with an order parameter of $\mathrm{d}_{x^2-y^2}$ symmetry.

5.1 s and d wave competition

The most general free energy density for an s-wave (ψ_s) and d-wave (ψ_d) with $d_{x^2-y^2}$ symmetry that transforms under $D_{4h} \times U(1) \times \mathcal{T}$ is given by

$$\begin{aligned} F = \int d^3x \Big[& a_1|\psi_s|^2 + b_1|\psi_s|^4 + k_1 |\mathbf{D}\psi_s|^2 + a_2|\psi_d|^2 + b_2|\psi_d|^4 + k_2 |\mathbf{D}\psi_d|^2 \\ & + \gamma_1|\psi_s|^2|\psi_d|^2 + \tfrac{1}{2}\gamma_2 \left(\psi_s^{*2}\psi_d{}^2 + \text{c.c.}\right) \\ & + \tfrac{1}{2}k_3 \left[(D_x\psi_s)^* (D_x\psi_d) - (D_y\psi_s)^* (D_y\psi_d) + \text{c.c.}\right] \Big]. \end{aligned} \tag{5.1}$$

We first express the order paramerters as $\psi_s = \psi_1 e^{i\phi_1}$ and $\psi_d = \psi_2 e^{i\phi_2}$, and reduce the problem to a one dimensional one to compare with our previous results. Considering the free energy deep

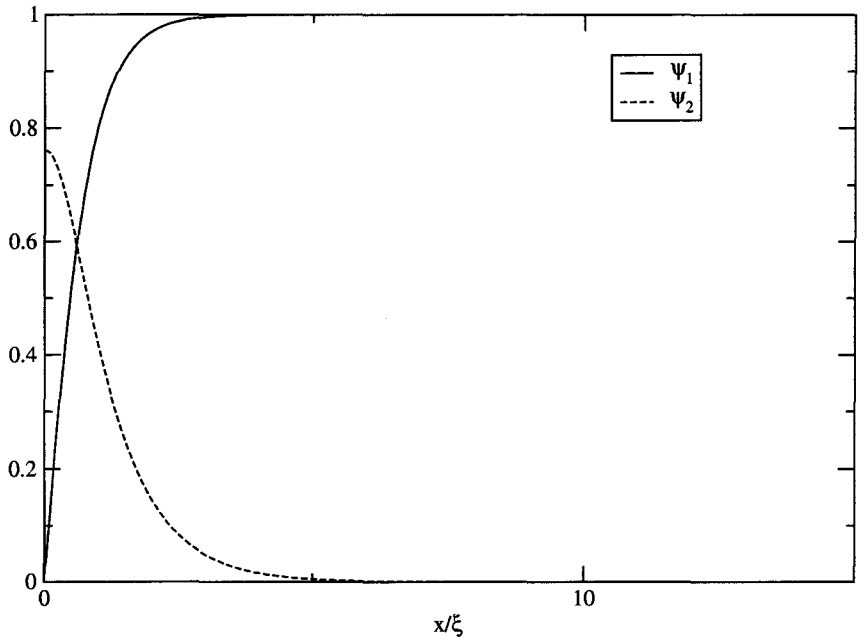

Figure 5.1: Order parameters showing the growth of the subdominant order parameter as the dominant order parameter is forced to zero by a boundary condition. The healing length of the dominant order parameter is not enlarged compared to the bare solution, and it is energetically unfavorable for the two order parameters to overlap for a large region. The parameters are given by $\frac{b_2}{b_1} = 1$, $\frac{k_2}{k_1} = 1$, $\frac{k_3}{k_1} = 1.6$, $\frac{\gamma_1 - \gamma_2}{b_1} = 1.9$, $\frac{T_{c2}}{T_{c1}} = 0.9$ and $\frac{T}{T_{c2}} = 0.9$.

inside the superconductor where the gradient vanish gives the following equations of motion:

$$0 = 2a_1\psi_1 + 4b_1\psi_1^3 + 2\gamma_1\psi_1\psi_2^2 + 2\gamma_2\psi_1\psi_2^2\cos(2(\phi_1 - \phi_2)), \tag{5.2}$$

$$0 = 2a_2\psi_2 + 4b_2\psi_2^3 + 2\gamma_1\psi_1\psi_1^2 + 2\gamma_2\psi_2\psi_1^2\cos(2(\phi_1 - \phi_2)), \tag{5.3}$$

$$0 = 2\gamma_2\psi_1^2\psi_2^2\sin(2(\phi_1 - \phi_2)). \tag{5.4}$$

This results in the condition $\phi_1 = \frac{\pi}{2} + \phi_2$ minimizing the free energy, as well as giving the magnitudes of the order parameters in the bulk:

$$\psi_1^2 = \frac{(\gamma_1 - \gamma_2)a_2 - 2a_1b_2}{4b_1b_2 - (\gamma_1 - \gamma_2)^2}, \tag{5.5}$$

$$\psi_2^2 = \frac{(\gamma_1 - \gamma_2)a_1 - 2a_2b_1}{4b_1b_2 - (\gamma_1 - \gamma_2)^2}. \tag{5.6}$$

These magnitudes assume that the temperature is low enough that both ψ_1 and ψ_2 have condensed. Without loss of generality we may assume that ψ_1 has a higher transition temperature.

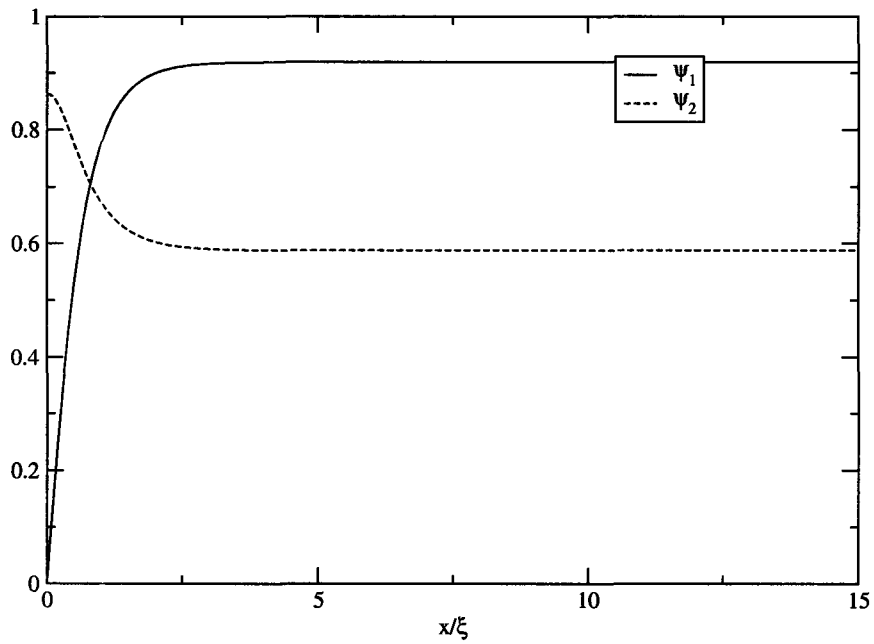

Figure 5.2: Here, we lower the energy cost for the order parameters to coexist. The dominant order parameter assumes a lower value in the bulk compared to it's bare value. The energy cost of coexisting with the dominant order parameter is cheaper than the gradient cost for having to increase in magnitude from zero. The parameters were given by $\frac{b_2}{b_1} = 1$, $\frac{k_2}{k_1} = 1$, $\frac{k_3}{k_1} = 1.6$, $\frac{\gamma_1 - \gamma_2}{b_1} = 0.9$, $\frac{T_{c2}}{T_{c1}} = 0.9$ and $\frac{T}{T_{c2}} = 0.9$.

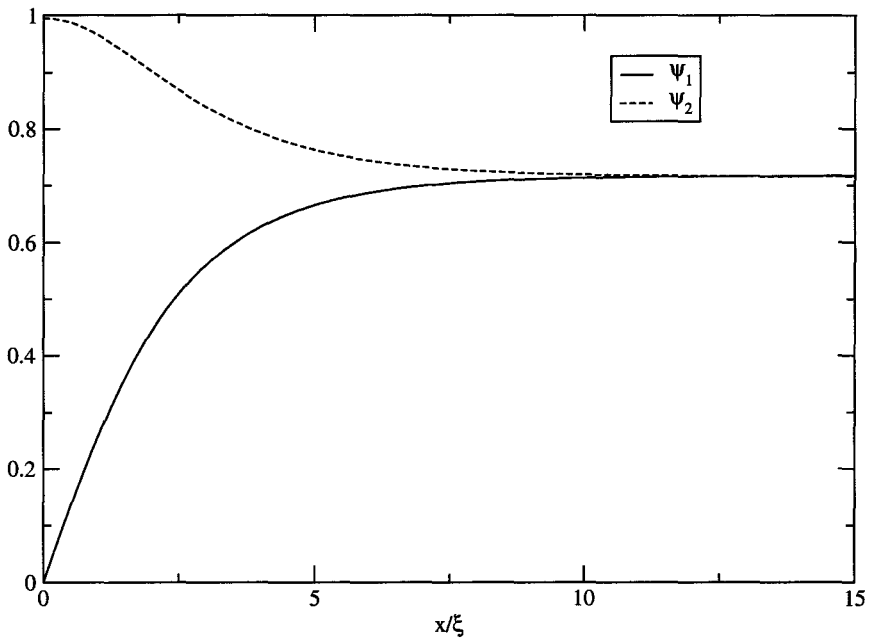

Figure 5.3: By tuning the transition temperatures closer together, both parameters attain the same value in the bulk and the influence of the order parameters on each other is the greatest. The parameters were given by $\frac{b_2}{b_1} = 1$, $\frac{k_2}{k_1} = 1$, $\frac{k_3}{k_1} = 1.6$, $\frac{\gamma_1 - \gamma_2}{b_1} = 0.9$, $\frac{T_{c2}}{T_{c1}} = 1$ and $\frac{T}{T_{c2}} = 0.9$

Then, the temperature at which the subdominant order parameter becomes non-zero is determined by the condition $(\gamma_1 - \gamma_2)a_1 - 2a_2b_1 = 0$.

In order study the effect of a subdominant order parameter on the shape and magnitude of the dominant order parameter, we scale the free energy by the bulk value of the dominant order in the absence of the sub dominant order, and the lengths by the coherence length of the bare dominant order parameter. In terms of the parameters in the free energy these are given by $\psi_1^2 = -\frac{a_1}{2b_1}$ and $\xi^s = \frac{2k_1}{a_1}$. The equations of motion were solved by the same Newton's method described in section 4.1. Some sample solutions are shown in Figs. 5.1, 5.2 and 5.3. In all of these solutions the dominant order was forced to zero at $x = 0$ with a boundary condition.

Below its transition temperature the subdominant order grows up, but has little effect on the dominant order. The dependance on all of the other free energy parameters only effects two things: the bulk value of the two order parameters, and the amount the subdominant order increased from this value. The only significant changes to the behaviour of the dominant order parameter was as the transition temperatures were tuned closer to one another. This is demonstrated for the limiting case in Fig. 5.3 where the transition temperatures assume equal values. In this case, the solution in the bulk is a superposition of the two states and this scenario will also change the properties of the bulk.

Given these results, we expect that the naive introduction of a competing order as a surface effect will likely have little change on the behaviour of the chiral p-wave order near the surface, and hence, on the currents. The situation will be somewhat different when the subdominant order is in the presence of a two component order parameter, and we turn to this possibility.

5.2 p-wave competition

To consider the effect of another order parameter which is favoured by the surface we add the following terms to the free energy:

$$f_2 = a_2|w|^2 + b_4|w|^4 + k_5\left(|D_x w|^2 + |D_y w|^2\right) + b_5|w|^2\left(|u|^2 + |v|^2\right) + b_6\left[w^{*2}\left(u^2 + v^2\right) + \text{c.c.}\right], \tag{5.7}$$

these terms would be caused by the addition of any one of the other unitary states allowed under the crystal symmetry. Here the new order parameter w is scaled by the bulk value of the chiral p-wave order. Notice, in particular, the lack of gradient terms coupling the new order parameters to the old ones. This lack of gradient terms can be proved by the following symmetry argument.

Let ψ_x and ψ_y be the x and y components of the chiral p-wave order parameter, and let ϕ be the new order parameter which is competing with them. The question is if there exist terms in the

free energy of the form:

$$(D_x\phi)^*(D_x\psi_x) + (D_x\phi)^*(D_x\psi_y) + \text{c.c.}$$

Where the D_x are the usual gauge covariant derivatives needed to maintain gauge invaiance. With terms like this in the free energy (with a large enough coupling constant) the ψ_x and ψ_y order parameters will be forced to heal on the same length scale as the ϕ order parameter. This could potentially reduce the surface currents, since these are caused by the different behaviour of ψ_x and ψ_y near the surface.

The equivalence of the x and y directions requires that these terms become:

$$(D_x\phi)^*(D_x\psi_x) + (D_x\phi)^*(D_x\psi_y) + (D_y\phi)^*(D_y\psi_y) + (D_y\phi)^*(D_y\psi_x) + \text{c.c.}$$

Now, using the symmetry $x \to -x$, the first (and fourth) term requires that ϕ be an odd function of x, whereas the second (and third) term requires that it is even. This leaves:

$$(D_x\phi)^*(D_x\psi_x) + (D_y\phi)^*(D_y\psi_x) + \text{c.c.}$$

Next, consider rotation by $\frac{\pi}{2}$ which takes $x \to y$ and $y \to -x$. This transformation, combined with the constraint from the previous symmetry operation that ϕ was odd in x, gives that these terms both map into their negative and hence cannot be included either.

Lastly, can any terms of the following form can be added?

$$(D_x\phi)^*(D_y\psi_y) + (D_y\phi)^*(D_x\psi_x) + \text{c.c.}$$

A term like this could suppress the magnitude of A_y in the presence of spatial variations of the new order parameter, ϕ. By applying $x \to -x$ it is immediately evident that the first term requires ϕ be odd while the second requires that it be even. Thus no such terms are allowed.

The lack of mixed gradient terms means that even when the parameters are such that this new order parameter can grow up near the surface, it has little effect on the shape of the old order parameters and hence, insignificant changes to the currents and fields.

To have a more significant impact on the field distribution we take the parameters that stabilize the chiral p-wave state to have spatial dependance. Instead of the introduction of a second order parameter we make a region close to the surface favour the $p_x + p_y$ state instead of the $p_x + ip_y$ state. In particular we change the sign of the b_2 term in the free energy in a region near the surface so that the phase changes as you move away from the surface into the bulk. The $p_x + p_y$ state does not have any spontaneously generated supercurrents and it being stabilized near the edge could reduce magnetic signatures. An advantage of this scenario, is that it ensures that the bulk maintains chiral p-wave order. The resulting currents and fields from a self-consistent calculation are shown in Fig.

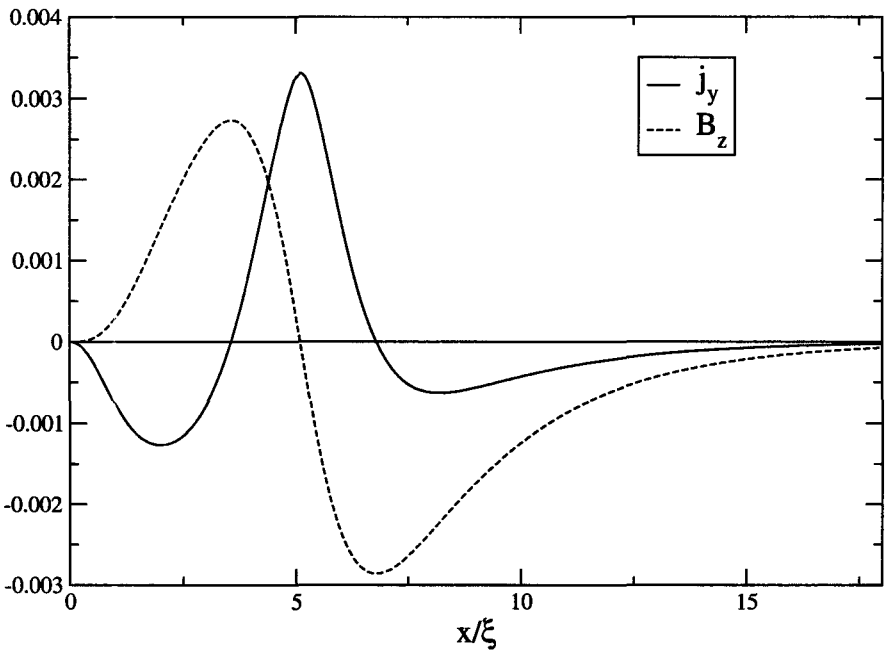

Figure 5.4: Computed currents and fields for a solution with varying phase. The parameters used are those for weak coupling, with b_2 negative for $x \leq 5$ but positive elsewhere.

5.4. Notice that both the overall magnitude of the fields is suppressed, as well as undergoing a change in sign. This alternating magnetic field is much like at a domain wall. The spatially alternating magnetic fields could reduce the measured signals since the magnetic probes are finite in size, but the overall change in field sign from the edge towards the bulk should still be measurable.

We lastly consider the effect of making the T_c of w in Eq. 5.7 larger than that of the chiral p-wave state in a region close to the edge. Self consistent solutions of the GL equations show that the new order parameter grows up at the surface, suppressing the chiral p-wave state which is recovered in the bulk. This configuration also gives rise to an alternating magnetic field, of similar magnitude to that shown in Fig. 5.4.

CHAPTER 6

Conclusions

In this thesis, we examined the discrepancy between the edge currents predicted as part of a chiral p-wave superconductor and the Hall bar [25] and scanning SQUID [26] measurements. The measurements indicating magnetism in the bulk [11, 12, 13] require that our description should produce bulk magnetic fields consistent with those taken to be attributed to domain walls. The effect of disorder alone at the surface was found to change the magnitude of the spontaneous magnetic signatures at the edge, but by far less than the upper bounds placed on the currents by Kirtley *et al.* [26] require. By examining the parameter space of the GL equations, we found that the parameter regimes which did not give rise to spontaneous currents were either devoid of any magnetic signatures, or corresponded to physically unlikely scenarios.

The effect of competing order near the surface was also investigated, and was found not to change the current significantly by changing the parameters in the GL equations alone. The largest effects were caused by the local T_c of the competing order parameter being higher than the bulk chiral p-wave T_c close to the edge, or by having the parameters which stabilize the chiral p-wave change in space so that it is not stable near the edge. The latter seems unlikely since these coefficients are usually functions of temperature, pressure, and other thermodynamic variables, although these parameters could change in the last few layers of the sample they will be unchanged over the relevant length scales (λ, ξ). In both cases, the field distribution is similar in nature to those produced at domain walls, and should be observable as the magnetic probes are moved from the edge towards the bulk.

These results provide evidence that the order in Sr_2RuO_4 may not be simply described by a chiral p-wave as was once suspected. Other measurements such as the Kerr effect, a sign of magnetism which was originally taken as evidence for chiral p-wave order is incompatible with a clean chiral p-wave superconductor [35, 36]. However, it was shown that impurities can generate a Kerr rotation

angle compatible with that observed [37]. Our calculation shows that disorder is insufficient to reduce the edge currents and it would be useful to have one model which captures all the physics of strontium ruthenate.

Recently, Leggett has proposed an alternative wavefunction that reduces to the BCS one for the case of spin singlet pairing [38]. While the BCS wavefunction predicts the angular momentum of the condensate of Cooper pairs to be given by [39, 19] $\frac{N\hbar}{2}$, the Leggett wavefunction instead gives that the angular momentum of the condensate is $\frac{N\hbar}{2}\left(\frac{\Delta}{\epsilon_f}\right)^2$. This large suppression of the angular momentum would indeed reduce spontaneous currents produced, but again, it is difficult to reconcile with the experimental signatures of broken time-reversal symmetry since one would naively expect the domain wall currents to be reduced as well. However, this requires a more careful examination of both the electromagnetic response and internal currents before this formulation can be ruled out. Nevertheless one may need to seek alternative explanations for the μSR and Josephson measurements which have been taken as evidence for domain walls in strontium ruthenate.

BIBLIOGRAPHY

[1] W. Kohn and J. M. Luttinger. New Mechanism for Superconductivity. *Physical Review Letters*, **15**(12), 1965.

[2] V.L. Ginzburg and L.D. Landau. *Zh. Eksperim. i Teor. Fiz.*, **20**:1064, 1950.

[3] L.D. Landau and E.M. Lifshitz. *Statistical Physics Volume 1.* Pergamon Press Ltd., 1980.

[4] L.P. Gor'kov. Microscopic Derivation of the Ginzburg-Landau Equations in the Theory of Superconductivity. *Sov. Phys. JETP*, **36**:1364, 1959.

[5] Y. Maeno, H. Hashimoto, K. Yoshida, S. Nishizaki, T. Fujita, J. G. Bednorz, and F. Lichtenberg. Superconductivity in a layered perovskite without copper. *Nature*, **372**(6506):532, 1994.

[6] P. W. Anderson. Theory of dirty superconductors. *Journal of Physics and Chemistry of Solids*, **11**(1-2):26, 1959.

[7] K. Ishida, H. Mukuda, Y. Kitaoka, K. Asayama, Z. Q. Mao, Y. Mori, and Y. Maeno. Spin-triplet superconductivity in Sr_2RuO_4 identified by 17O Knight shift. *Nature*, **396**(6712):658, 1998.

[8] K. Ishida, H. Mukuda, Y. Kitaoka, Z. Q. Mao, H. Fukazawa, and Y. Maeno. Ru NMR probe of spin susceptibility in the superconducting state of Sr_2RuO_4. *Phys. Rev. B*, **63**(6):060507, 2001.

[9] J. A. Duffy, S. M. Hayden, Y. Maeno, Z. Mao, J. Kulda, and G. J. McIntyre. Polarized-Neutron Scattering Study of the Cooper-Pair Moment in Sr_2RuO_4. *Phys. Rev. Lett.*, **85**(25):5412, 2000.

[10] K. D. Nelson, Z. Q. Mao, Y. Maeno, and Y. Liu. Odd-Parity Superconductivity in Sr_2RuO_4. *Science*, **306**(5699):1151, 2004.

[11] G. M. Luke, Y. Fudamoto, K. M. Kojima, M. I. Larkin, J. Merrin, B. Nachumi, Y. J. Uemura, Y. Maeno, Z. Q. Mao, Y. Mori, H. Nakamura, and M. Sigrist. Time-reversal symmetry-breaking superconductivity in Sr_2RuO_4. *Nature*, **394**(6693):558, 1998.

[12] G. M. Luke, Y. Fudamoto, K. M. Kojima, M. I. Larkin, B. Nachumi, Y. J. Uemura, J. E. Sonier, Y. Maeno, Z. Q. Mao, Y. Mori, and D. F. Agterberg. Unconventional superconductivity in Sr_2RuO_4. *Physica B: Condensed Matter*, **289-290**:373, 2000.

[13] Francoise Kidwingira, J. D. Strand, D. J. Van Harlingen, and Yoshiteru Maeno. Dynamical Superconducting Order Parameter Domains in Sr_2RuO_4. *Science*, **314**(5803):1267, 2006.

[14] Jing Xia, Yoshiteru Maeno, Peter T. Beyersdorf, M. M. Fejer, and Aharon Kapitulnik. High Resolution Polar Kerr Effect Measurements of Sr_2RuO_4: Evidence for Broken Time-Reversal Symmetry in the Superconducting State. *Phys. Rev. Lett.*, **97**(16):167002, 2006.

[15] T.M. Rice and M. Sigrist. Sr_2RuO_4: an electronic analogue of ^{3}He? *J. Phys. Cond. Matter*, **7**:L643, 1995.

[16] G. E. Volovik. An analog of the quantum Hall effect in a superfluid ^{3}He film. *Sov. Phys. JETP*, **67**:1804, 1988.

[17] Andrew Peter Mackenzie and Yoshiteru Maeno. The superconductivity of Sr_2RuO_4 and the physics of spin-triplet pairing. *Rev. Mod. Phys.*, **75**(2):657, 2003.

[18] Maurice Rice. Physics: Superconductivity with a Twist. *Science*, **314**(5803):1248, 2006.

[19] Michael Stone and Rahul Roy. Edge modes, edge currents, and gauge invariance in $p_x + ip_y$ superfluids and superconductors. *Phys. Rev. B*, **69**(18):184511–12, 2004.

[20] M. Matsumoto and M. Sigrist. Quasiparticle States near the Surface and the Domain Wall in a $p_x \pm ip_y$. *J. Phys. Soc. Jpn.*, **68**(3):944, 1999.

[21] Manfred Sigrist and Kazuo Ueda. Phenomenological theory of unconventional superconductivity. *Rev. Mod. Phys.*, **63**(2):239, 1991.

[22] M. Sigrist, T. M. Rice, and K. Ueda. Low-field magnetic response of complex superconductors. *Phys. Rev. Lett.*, **63**(16):1727, 1989.

[23] Akira Furusaki, Masashige Matsumoto, and Manfred Sigrist. Spontaneous Hall effect in a chiral p-wave superconductor. *Phys. Rev. B*, **64**(5):054514, 2001.

[24] Hyok-Jon Kwon, Victor M. Yakovenko, and K. Sengupta. How to detect edge electron states in (TMTSF)2X and Sr_2RuO_4 experimentally. *Synthetic Metals*, **133-134**:27, 2003.

[25] Per G. Bjornsson, Yoshiteru Maeno, Martin E. Huber, and Kathryn A. Moler. Scanning magnetic imaging of Sr_2RuO_4. *Phys. Rev. B*, **72**(1):012504, 2005.

[26] J. R. Kirtley, C. Kallin, C. W. Hicks, E. A. Kim, Y. Liu, K. A. Moler, Y. Maeno, and K. D. Nelson. Upper limit on spontaneous supercurrents in Sr_2RuO_4. *Phys. Rev. B*, **76**(1):014526, 2007.

[27] A. P. Mackenzie, R. K. W. Haselwimmer, A. W. Tyler, G. G. Lonzarich, Y. Mori, S. Nishizaki, and Y. Maeno. Extremely Strong Dependence of Superconductivity on Disorder in Sr_2RuO_4. *Phys. Rev. Lett.*, **80**(1):161, 1998.

[28] Yasushi Nagato, Mikio Yamamoto, and Katsuhiko Nagai. Rough Surface Effects on the p-Wave Fermi Superfluids. *J. Low Temp. Phys.*, **110**(5):1135, 1998.

[29] J. Dimmock R. wheeler G. Koster and H. Statz. *Properties of the Thrty-two Point Groups.* M.I.T. Press, 1963.

[30] Michael Tinkham. *Group Theory and Quantum Mechanics.* Dover Publications Inc., 2003.

[31] V.P. Mineev and K.V. Samokhin. *Introduction to Unconventional Superconductivity.* Gordon and Breach Science Publishers, 1999.

[32] P. G. deGennes. *Superconductivity of Metals and Alloys.* Benjamin, New York, 1966.

[33] V. Ambegaokar, P. G. deGennes, and D. Rainer. Landau-Ginsburg equations for an anisotropic superfluid. *Phys. Rev. A*, **9**(6):2676, 1974.

[34] E. V. Thuneberg. Ginzburg-Landau theory of vortices in superfluid^{3}He-B. *Phys. Rev. B*, **36**(7):3583, 1987.

[35] Rahul Roy and Catherine Kallin. Collective modes and electromagnetic response of a chiral superconductor. *Phys. Rev. B*, **77**(17):174513, 2008.

[36] Roman M. Lutchyn, Pavel Nagornykh, and Victor M. Yakovenko. Gauge-invariant electromagnetic response of a chiral $p_x + ip_y$ superconductor. *Phys. Rev. B*, **77**(14):144516, 2008.

[37] Jun Goryo. Impurity-induced polr Kerr effect in a chiral p-wave superconductor. *Phys. Rev. B*, **78**(6):060501, 2008.

[38] A.J. Legget. *Quantum Liquids.* Oxford University Press, 2007.

[39] N. D. Mermin and Paul Muzikar. Cooper pairs versus Bose condensed molecules: The ground-state current in superfluid He3-A. *Phys. Rev. B*, **21**(3):980, 1980.